synapses without any stimulation, and this phenomenon can be visualized as periodic changes in the concentration of intracellular Ca^{2+} (synchronous oscillation) (Yasumoto *et al.*, 2004). The cultured midbrain neurons conform their networks step by step according to the days in vitro (DIV) and increase the frequency of spontaneous synchronous oscillation gradually (data not shown). Because of these characteristics, this neural network-generating synchronous oscillation is considered to be a good in vitro model of a developing CNS. In our previous study, we also confirmed that endogenous dopamine regulated synchronous oscillation via dopamine receptors (DRs), and the regulation was distinctly different through two DR families, dopamine receptor 1 and 2 (D1R and D2R, respectively): dopamine through D1R was facilitative to the Ca^{2+} influx of synchronous oscillation, while that through D2R was suppressive to it.

In the present study, we investigated the mechanisms of this suppressive regulation by D2R of the Ca^{2+} influx in the primary cultured midbrain neural network. Two major Ca^{2+} channels are reported to be affected by D2R, the L-type voltage-gated Ca^{2+} channel and a ligand-gated Ca^{2+} channel, the N-methyl-D-aspartate receptor (NMDAR) (Cepeda *et al.*, 1998). However, the changes of intracellular Ca^{2+} concentrations mediated by the activation or inactivation of D2R reported previously did not have much relation with the neural activity induced naturally by endogenous dopamine and may not influence the dynamics essential for neural development. This is the first report describing the interaction of D2R with the L-type voltage-gated Ca^{2+} channel, but not with NMDAR, with regard to the suppressive effects on the Ca^{2+} influx in the midbrain neural network showing synchronous oscillation.

MATERIALS AND METHODS

Animals

Pregnant ICR mice were purchased from SLC (Shizuoka, Japan) and maintained under controlled conditions (temperature, 24 ± 1°C; humidity, 55 ± 5%). They were fed a commercial diet of CMF (Oriental Yeast, Tokyo, Japan) and tap water, both provided ad libitum. This experiment was performed in accordance with the Guidelines for Animal Experimentation, The University of Tokyo, and was approved by The Institutional Animal Care and Use Committee of The Graduate School of Agricultural and Life Sciences, The University of Tokyo.

Primary culture of neurons from midbrain

Primary cultures of neurons were performed according to a previously reported method (Yasumoto *et al.*, 2004). Fetuses were removed at gestational day 17, and isolated fetal midbrains were cut into small pieces in isolation medium (equal volumes of Dulbecco's Modified Eagle's Medium (DMEM) (Sigma, St. Louis, MO) and Ca^{2+} and Mg^{2+}-free phosphate-buffered saline (PBS)). Small pieces of midbrain were digested by 11.2 units/ml dispase, and cells in culture medium (DMEM with 10% horse serum) were plated at 1.1×10^4 cells/mm^2 on polyethylenimine (PI) (Sigma)

coated glass coverslips. All cultured cells were maintained in a humidified atmosphere of 95% air and 5% CO_2 at 37°C.

Intracellular Ca^{2+}recording

Measurement of the intracellular Ca^{2+} concentration was carried out at 7-8 DIV culture according to a previously reported procedure (Ogura *et al.*, 1987). Briefly, cells were loaded with 5μM fura-2-AM (Dojin, Kumamoto, Japan) in balanced salt solution (BSS), randomly chosen by 10 × 10-μm squares, and the ratios of intensity at 340 and 360 nm, which corresponded to changes in the intracellular Ca^{2+} concentrations of individual cells, were recorded by the Argus-50 system (Hamamatsu Photonics, Hamamatsu, Japan).

Chemicals

R(-)-2-amino-5-phosphonopentanoic acid (AP5) (Sigma), nifedipine (Latoxan), and raclopride (Sigma) were used, respectively, as an NMDAR antagonist, a L-type voltage-gated Ca^{2+} channel antagonist, and a D2R antagonist. AP5 (10 mM) was dissolved in purified water, nifedpipine (10 mM) in dimethylsulfoxide (DMSO), and raclopride (1 mM) in BSS, respectively, for storage. All chemicals were diluted in BSS to the working concentrations indicated and quickly administered by pipette situated just above the liquid level. We did not observe any detectable effect of any of the vehicles on intracellular Ca^{2+}(data not shown).

RESULTS

The concentration of intracellular Ca^{2+} in cultured midbrain neurons, as visualized by fura-2 (Fig. 1A), changed synchronously and periodically without any stimulation (synchronous oscillation) at 7-8 DIV (Fig. 1B). Raclopride (10 μM), a selective D2R antagonist, induced a transient increase in intracellular Ca^{2+} concentration and synchronous oscillation disappeared (number of separate cultures (Nc) = 4, number of total wells examined (Nw) = 7, 49/49 (cells responded to the chemical/examined cells), Fig. 1C).

AP-5 (100 μM), an NMDAR antagonist (Nc = 4, Nw = 4, 28/28 cells, Fig. 2A) and nifedipine (100 μM), an L-type voltage-gated Ca^{2+} channel antagonist (Nc = 4, Nw = 8, 56/56 cells, Fig. 2B) both inhibited synchronous oscillation. Although raclopride (10 μM), even in the presence of AP-5 (100 μM), induced a transient increase of intracellular Ca^{2+}(Nc = 4, Nw = 4, 28/28 cells, Fig. 2A), raclopride (10 μM) in the presence of nifedipine (100 μM) failed to induce a transient increase of intracellular Ca^{2+} (Nc = 4, Nw = 8, 56/56 cells, Fig. 2B).

DISCUSSION

Our previous report verified that synchronous oscillation of midbrain neurons was accompanied by membrane depolarizations and action potentials through functional glutamatergic synapses of neurons, and this phenomenon was considered to

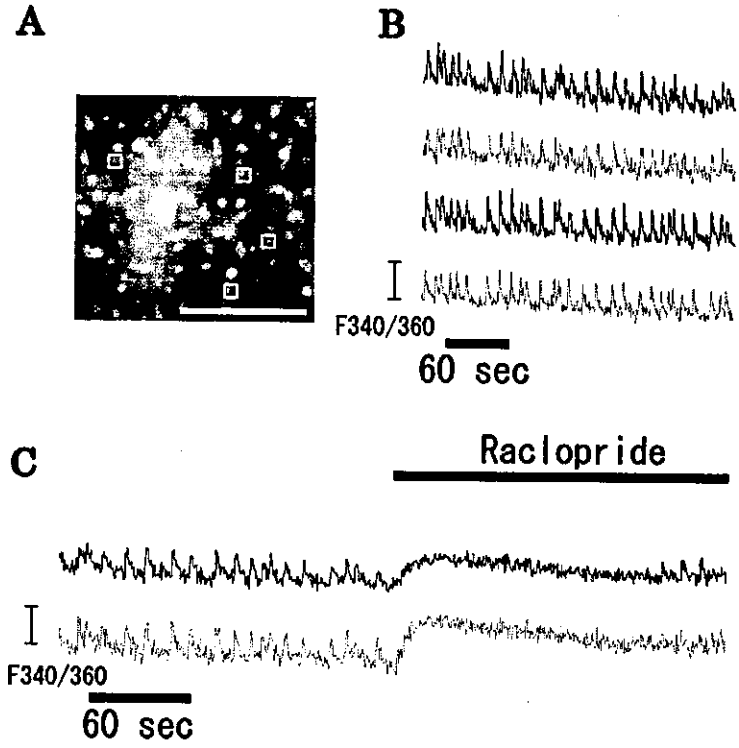

Fig. 1. Midbrain nerous at 7 DIV were visualized by loading fura-2 (A), and each labeled neuron showed synchronous oscillations of intracellular Ca^{2+} concentration (B). Raclopride (10 μM) induced a transient increase of intracellular $Ca^{2+}$and inhibited synchronous oscillation of cultured midbrain neurons (C). Scale bar represents 100 μm in (A).

reflect neural development in the CNS (Yasumoto *et al.*, 2004). In the present study, we further confirmed that synchronous oscillation of midbrain neurons was generated by the Ca^{2+}influx through the L-type voltage-gated Ca^{2+} channel, because nifedipine, an L-type voltage-gated Ca^{2+} channel antagonist, inhibited synchronous oscillation.

Previously, we also confirmed that synchronous oscillation of midbrain neurons was regulated by dopamine, which was distinct from synchronous oscillation of cortical neurons. D1R and D2R had different roles in synchronous oscillation; the action of endogenous dopamine through D1R was facilitative to the Ca^{2+} influx of synchronous oscillation, and that through D2R was suppressive to the Ca^{2+} influx. In addition, our present results suggest that signals of endogenous dopamine through D2R suppress the activation of the L-type voltage-gated Ca^{2+} channel. In general, D2R is said to relate to both the L-type voltage-gated Ca^{2+} channel and NMDAR (Cepeda *et al.*, 1998; Flores-Hernandez *et al.*, 2002). In the present study, however, we excluded the interaction of D2R with NMDAR in primary cultured midbrain neural network generating synchronous oscillation. This discordance might result from the difference in the method of applying dopamine: we used spontaneously released endogenous dopamine in the present study versus bath-applied dopamine-agonists

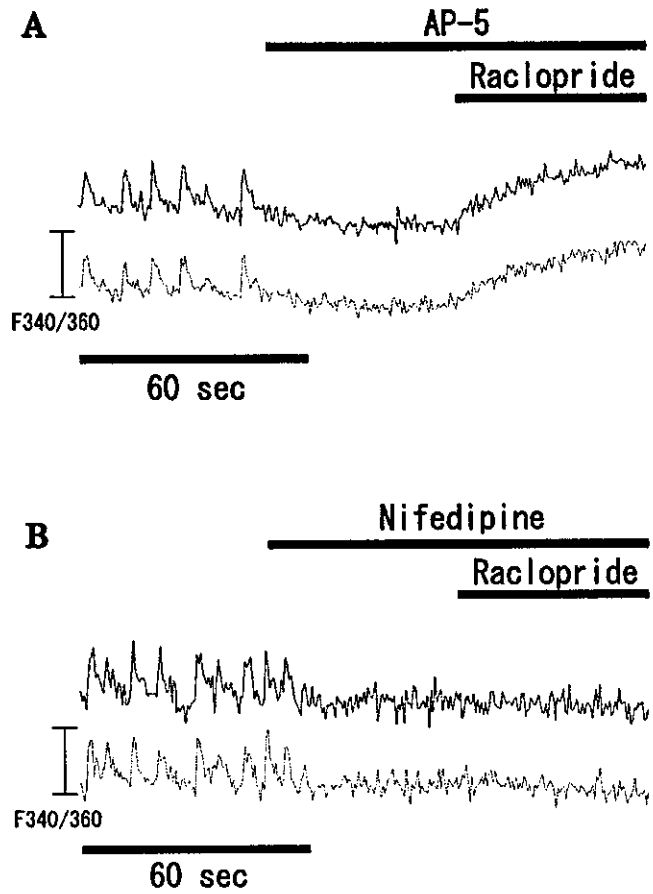

Fig. 2. (A) AP-5 (100 μM) inhibited synchronous oscillation of midbrain neurons. Raclopride (10 μM) in the presence of AP-5 (100 μM) induced a transient increase of intracellular Ca^{2+} as same as it was applied alone. (B) Nifedipine (100 μM) inhibited synchronous oscillation of midbrain neurons. Raclopride (10 μM) in the presence of nifedipine (100 μM) did not induce a transient increase of intracellular Ca^{2+}.

in the previous studies (Cepeda *et al.*, 1998; Flores-Hernandez *et al.*, 2002). Bath-applied dopaminergic drugs act on the DRs in both extra- and intrasynapses, while endogenous dopamine acts mainly on intrasynaptic DRs. Based on the present result, D2R in intrasynapses, unlike that in extrasynapses, might have little interaction with NMDAR, which probably reflects the *in vivo* function of D2R in the developing CNS more appropriately.

We cannot eliminate the possibility that dopamine release is inhibited by blocking of the L-type voltage-gated Ca^{2+} channel but not by blocking of NMDAR, which resulted in the inefficaciousness of raclopride in the presence of nifedipine. And endogenous dopamine release might be independent of the activation of NMDAR, e.g., in synchronous oscillation, as dopamine was still released in the presence of AP-5 and acted on D2R. Further investigation assessing dopamine release is needed.

The results of the present study clarifying the mechanism of suppressive regulation by D2R of the Ca^{2+} influx may promote better understanding of the regulation of neural activity by endogenous dopamine and the developing dopaminergic neural networks.

REFERENCES

Cepeda, C., Colwell, C. S., Itri, J. N., Chandler, S. H., and Levine, M. S. (1998). Dopaminergic modulation of NMDA-induced whole cell currents in neostriatal neurons in slices: contribution of calcium conductances. *J. Neurophysiol.* **79**:82–94.

Flores-Hernandez, J., Cepeda, C., Hernandez-Echeagaray, E., Calvert, C. R., Jokel, E. S., Fienberg, A. A., Greengard, P., and Levine, M. S. (2002). Dopamine enhancement of NMDA currents in dissociated medium-sized striatal neurons: role of D1 receptors and DARPP-32. *J. Neurophysiol.* **88**:3010–3020.

Garaschuk, O., Hanse, E., and Konnerth, A. (1998). Developmental profile and synaptic origin of early network oscillations in the CA1 region of rat neonatal hippocampus. *J. Physiol. (Lond.)* **507**:219–236.

Gray, C. M., Konig, P., Engel, A. K., and Singer, W. (1989). Oscillatory responses in cat visual cortex exhibit inter-columnar synchronization which reflects global stimulus properties. *Nature* **338**:334–337.

Nakamura, K., Mikami, A., and Kubota, K. (1992). Oscillatory neuronal activity related to visual short-term memory in monkey temporal pole. *Neuroreport* **3**:117–120.

Ogura, A., Iijima, T., Amano, T., and Kudo, Y. (1987). Optical monitoring of excitatory synaptic activity between cultured hippocampal neurons by a multi-site Ca2+ fluorometry. *Neurosci. Lett.* **78**:69–74.

Yasumoto, F., Negishi, T., Ishii, Y., Kyuwa, S., Kuroda, Y., and Yoshikawa, Y. (2004). Endogenous dopamine maintains synchronous oscillation of intracellular calcium in primary cultured-mouse midbrain neurons. *Cell. Mol. Neurobiol.* **24**:51–61.

Cellular and Molecular Neurobiology, Vol. 24, No. 6, December 2004 (© 2004)

Glutamate Regulates the Frequency of Spontaneous Synchronized Ca^{2+} Spikes Through Group II Metabotropic Glutamate Receptor in Cultured Mouse Cortical Networks

Fumie Yasumoto,[1,3,4] Takayuki Negishi,[1,3] Yoshiyuki Ishii,[1] Shigeru Kyuwa,[1] Yoichiro Kuroda,[2,3] and Yasuhiro Yoshikawa[1,3]

Received April 19, 2004; accepted May 6, 2004

SUMMARY

1. Synchronized spontaneous intracellular Ca^{2+} spikes in networked neurons are believed to play a major role in the development and plasticity of neural circuits. Glutamate-induced signals through the ionotropic glutamate receptors (iGluRs) are profoundly involved in the generation of synchronized Ca^{2+} spikes.

2. In this study, we examined the involvement of metabotropic glutamate receptors (mGluRs) in cultured mouse cortical neurons. We pharmacologically revealed that glutamate-induced signals through inclusive mGluRs decreased the frequency of Ca^{2+} spikes. Further experiments indicated that this suppressive effect on the spike frequency was mainly due to the signal through group II mGluR, inactivation of adenylate cyclase-cAMP-PKA signaling pathway. Group I mGluR had little involvement in the spike frequency.

3. Taken together, glutamate generates the synchronized Ca^{2+} spikes through iGluRs and modulates simultaneously their frequency through group II mGluR–adenylate cyclase–cAMP–PKA signaling pathway in the present *in vitro* neural network. These results provide the evidence of the profound role of group II mGluR in the spontaneous and synchronous neural activities.

KEY WORDS: mGluRs; PKA; synaptic transmission; Ca^{2+} imaging; synchronized Ca^{2+} spikes.

[1] Department of Biomedical Science, Graduate School of Agricultural and Life Sciences, The University of Tokyo, Yayoi, Bunkyo-ku, Tokyo, Japan.
[2] Department of Molecular and Cellular Neurobiology, Tokyo Metropolitan Institute for Neuroscience, Musashidai, Fuchu, Tokyo, Japan.
[3] Core Research for Evolutional Science and Technology, Japan Science and Technology Corporation, Kawaguchi-shi, Saitama, Japan.
[4] To whom correspondence should be addressed at Department of Biomedical Science, Graduate School of Agricultural and Life Sciences, The University of Tokyo, 1-1-1 Yayoi, Bunkyo-ku, Tokyo 113-8657, Japan; e-mail: aa37169@mail.ecc.u-tokyo.ac.jp.

0272-4340/04/1200-0841/0

INTRODUCTION

Neurons in the central nervous system (CNS) change intracellular calcium synchronously and periodically, which is accompanied by neural bursts through glutamatergic synapses, and this oscillatory phenomenon is believed to be essential to the development and differentiation of the CNS (Garaschuk *et al.*, 1998; Gray *et al.*, 1989; Nakamura *et al.*, 1992). It is known that primary cultured rat cortical neurons also burst synchronously and periodically through glutamatergic synapses (Robinson *et al.*, 1993) without any stimulation, and this phenomenon can be visualized as periodic changes in the concentrations of intracellular Ca^{2+} (Kuroda *et al.*, 1992). This phenomenon is therefore considered to be a good *in vitro* model of synchronized Ca^{2+} spikes in the developing CNS.

Glutamate, the major excitatory neurotransmitter, stimulates two types of glutamate receptors: ionotropic glutamate receptors (iGluRs), which are ligand-gated ion channels and regulate synaptic response, and metabotropic glutamate receptors (mGluRs) (Nakanishi, 1992). Kuroda *et al.* have found that synchronized spontaneous intracellular Ca^{2+} spikes are generated by the glutamate-induced responses through iGluRs. However, the regulatory mechanism of mGluRs in these synchronized Ca^{2+} spikes remains unclear. In the present study, we examined the role of the signals through mGluRs, focusing on the frequency changes of synchronized Ca^{2+} spikes.

mGluRs consist of at least eight subtypes that regulate a variety of intracellular signaling systems via the activation of guanosine triphosphate (GTP)-binding proteins (Pin and Duvoisin, 1995; Schoepp *et al.*, 1999). These subtypes have been subdivided into three main groups: group I mGluR (consisting of mGluR1 and 5) functionally couples to phospholipase C and affects the PKC signaling pathway; groups II (mGluR2 and 3) and III (mGluR4, 6, 7, and 8) mGluRs inhibit adenylate cyclase, mediate a decrease in cAMP concentrations, and thereby inhibit the protein kinase A (PKA) cascade (Schoepp *et al.*, 1999). According to some reports, mGluRs are profoundly involved in various synaptic transmissions, and also influence the long-lasting activity-dependent changes in excitatory glutamatergic transmission, long-term depression (LTD), and long-term potentiation (LTP) (Manahan-Vaughan, 1997).

We report here for the first time that glutamate is involved not only in the generation of synchronized Ca^{2+} spikes through iGluRs, but also in the regulation of frequency in synchronized Ca^{2+} spikes through the activation of group II mGluR.

MATERIALS AND METHODS

Animals

Pregnant ICR mice were purchased from SLC (Shizuoka, Japan) and maintained under controlled conditions (temperature, 24 ± 1°C; humidity, 55 ± 5%). They were fed a commercial diet of CMF (Oriental Yeast, Tokyo, Japan) and tap water, both provided *ad libitum*. This experiment was performed in accordance with the Guidelines for Animal Experimentation, The University of Tokyo, and was approved

by The Institutional Animal Care and Use Committee of The Graduate School of Agricultural and Life Sciences, The University of Tokyo.

Primary Culture of Neurons From Cerebral Cortices

Primary cultures of cortical neurons were performed according to a previously reported method (Ichikawa *et al.*, 1993; Yasumoto *et al.*, 2004). Fetuses were removed at gestational day 17 and isolated fetal cerebral cortices were cut into small pieces in isolation medium (equal volumes of Dulbecco's Modified Eagle's Medium (DMEM) (Sigma, St. Louis, MO) and Ca^{2+}- and Mg^{2+}-free phosphate-buffered saline (PBS)). Small pieces of cerebral cortices were digested by 11.2 units/mL dispase, and cells in culture medium (DMEM with 10% horse serum) were plated at 1.1×10^4 cells/mm^2 on polyethylenimine (PI) (Sigma) coated glass coverslips. All cultured cells were maintained in a humidified atmosphere of 95% air and 5% CO_2 at 37°C.

Intracellular Calcium Recording

Measurement of intracellular Ca^{2+} concentrations was carried out at 7–9 days *in vitro* (DIV) according to a previously reported procedure (Ogura *et al.*, 1987). Briefly, cells were loaded with 10 μM fura-2-AM (Dojin, Kumamoto, Japan) in balanced salt solution (BSS), randomly chosen by 10×10 μm squares, and the ratios of intensity at 340 and 360 nm, which corresponded to changes in the intracellular Ca^{2+} concentrations of individual cells, were recorded by the Argus-50 system (Hamamatsu Photonics, Hamamatsu, Japan).

Chemicals

Tetrodotoxin (TTX) (Sigma) was used as a voltage-dependent Na^+ channel inhibitor. (+)−α-methyl-4-carboxyphenylglycine (MCPG) (Sigma) and *trans*-(1*S*,3*R*)-1-amino-1,3-cyclopentanedicarboxylic acid (ACPD) (Sigma) were used as a wide-spectrum mGluRs antagonist and a wide-spectrum mGluRs agonist, respectively. 1-Amino-2,3-dihydro-1H-indene-1,5-dicarboxylic acid (AIDA) (Sigma) and *N*-phenyl-7-(hydroxyimino)cyclopropa [*b*] chromen-1a-carboxamide (PHCCC) (Tocris) were both used as group I mGluR antagonists, and (2*S*)-α-ethylglutamic acid (EGLU) (Tocris) was used as a group II mGluR antagonist. Protein kinase A (PKA) inhibitor fragment 14–22 (PKI(14–22)) (Sigma) and forskolin (Sigma) were used as a PKA inhibitor and a adenylate cyclase activator, respectively.

TTX (100 μM), ACPD (10 mM), AIDA (10 mM), and PKI(14–22) (1 mM) were all dissolved in sterilized BSS for storage. MCPG (50 mM) and EGLU (100 mM) were prepared from a stock solution dissolved in 0.1 M and 1 M NaOH, respectively. PHCCC (3 mM) was dissolved in dimethylsulfoxide (DMSO) for storage. Forskolin (7.5 mM) was dissolved in ethanol for storage. All chemicals were diluted in BSS (prewarmed to 37°C) to the working concentrations indicated, and quickly administered by pipette situated just above the liquid level, and then chemicals in BSS were perfused.

To quantify the changes in the frequency of Ca^{2+} spikes in response to chemicals, we counted the number of Ca^{2+} spikes for 2.5 min prior to (pre) and after (post) chemicals application, and the ratio of frequency (post/pre) was calculated. We confirmed that various vehicles, as the controls described above, did not change the frequency of the synchronized Ca^{2+} spikes and the ratio values were almost 1.0 as indicated for the controls in each figure. These results indicated that no artifact was produced by the bath application method.

The working concentrations of chemicals were decided upon according to previous researches, as follows. TTX (1 μM) (Yasumoto *et al.*, 2004), ACPD (5–100 μM), and MCPG (500 μM) (Schwarz *et al.*, 2000), AIDA (100 μM) (Kalda *et al.*, 2000), PHCCC (30 μM (Thornton and Bornstein, 2002), EGLU (300 μM (Marti *et al.*, 2001), PKI(14–22) (0.05–50 mM) (Sluka, 1997), and forskolin (1–30 μM (Akasu and Tokimasa, 1989) were all effective in each study. In many previous researches, AIDA (Aguirre *et al.*, 2001; Meli *et al.*, 2002; Zhou *et al.*, 2001) and PHCCC (Maj *et al.*, 2003; Mao and Wang, 2001a,b) have often used at concentrations lower than 100 or 30 μM, respectively.

Statistics

All numerical values were represented as means ± SD, and the differences between experimental groups were evaluated using the Student's *t* test. In all cases, a probability value of <0.05 was considered statistically significant.

RESULTS

Synchronized Intracellular Ca^{2+} Spikes in Primary Cultured Mouse Cortical Neurons

Periodic and spontaneous synchronized Ca^{2+} spikes in cultured rat CNS neurons have been reported previously, and have been found to involve action-potential firings among synaptically connected neurons (Bacci *et al.*, 1999; Numakawa *et al.*, 2002; Przewlocki *et al.*, 1999; Verderio *et al.*, 1999). Furthermore, concurrent recordings of membrane potentials and intracellular Ca^{2+} concentrations have revealed that each Ca^{2+} spike correlates to a burst of action potentials (Bacci *et al.*, 1999; Verderio *et al.*, 1999). The concentrations of intracellular Ca^{2+} in the present cultured mouse cortical cells, as visualized by fura-2 (Fig. 1(A)), changed synchronously and periodically without any stimulation at 7–9 DIV (Fig. 1(B)). To confirm that these Ca^{2+} spikes were driven by membrane depolarization through action potentials, we applied tetrodotoxin (TTX) to block neural action potentials. We found that TTX (1 μM) completely abolished all Ca^{2+} spikes (number of separate cultures (Nc) = 4, number of total wells examined (Nw) = 4, 28/28 (cells responded to the chemical/examined cells), Fig. 1(C)), indicating that these Ca^{2+} spikes were the direct results of membrane depolarization from action potentials among synaptically connected neurons.

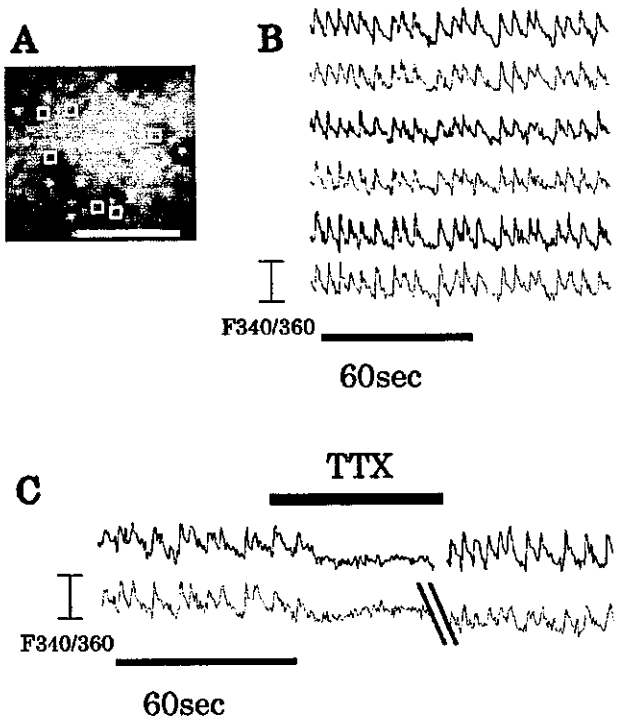

Fig. 1. Synchronized spontaneous intracellular Ca^{2+} spikes in primary cultured mouse cortical neurons. Cortical neurons at 8 DIV were visualized by loading fura-2 (A), and each labeled neuron showed synchronized spontaneous intracellular Ca^{2+} spikes (B). Scale bar in (A) represents 100 μm. TTX (1 μM) inhibited synchronized the Ca^{2+} spikes of cortical neurons at 8 DIV in a reversible manner (C). The time gap (//) was 150 s.

Signals Through mGluRs Negatively Regulate the Frequency of Synchronized Ca^{2+} Spikes in Cultured Mouse Cortical Neurons

To investigate the effects of mGluRs on synchronized Ca^{2+} spikes, we bath-applied pharmacological agents known to affect the signaling pathways of mGluRs, and recorded the frequency of synchronized Ca^{2+} spikes before and after drug application. MCPG (500 μM), a wide-spectrum mGluR antagonist, induced a significant increase in the frequency of synchronized Ca^{2+} spikes (Nc = 5, Nw = 6, 42/42 cells, Fig. 2(A) and (B)). This result suggested that there was endogenous activation of mGluRs in untreated cortical cultures, and that the effects of inclusive mGluRs were suppressive to the frequency of synchronized Ca^{2+} spikes. In contrast, ACPD (10 μM), a wide-spectrum mGluR agonist, induced a significant decrease in the frequency of synchronized Ca^{2+} spikes (Nc = 5, Nw = 6, 42/42 cells, Fig. 2(C) and (D)). These results strongly suggest that glutamate signals through mGluRs regulated the frequency of synchronized Ca^{2+} spikes in neural networks, and that signals through inclusive mGluRs depress the frequency of Ca^{2+} spikes.

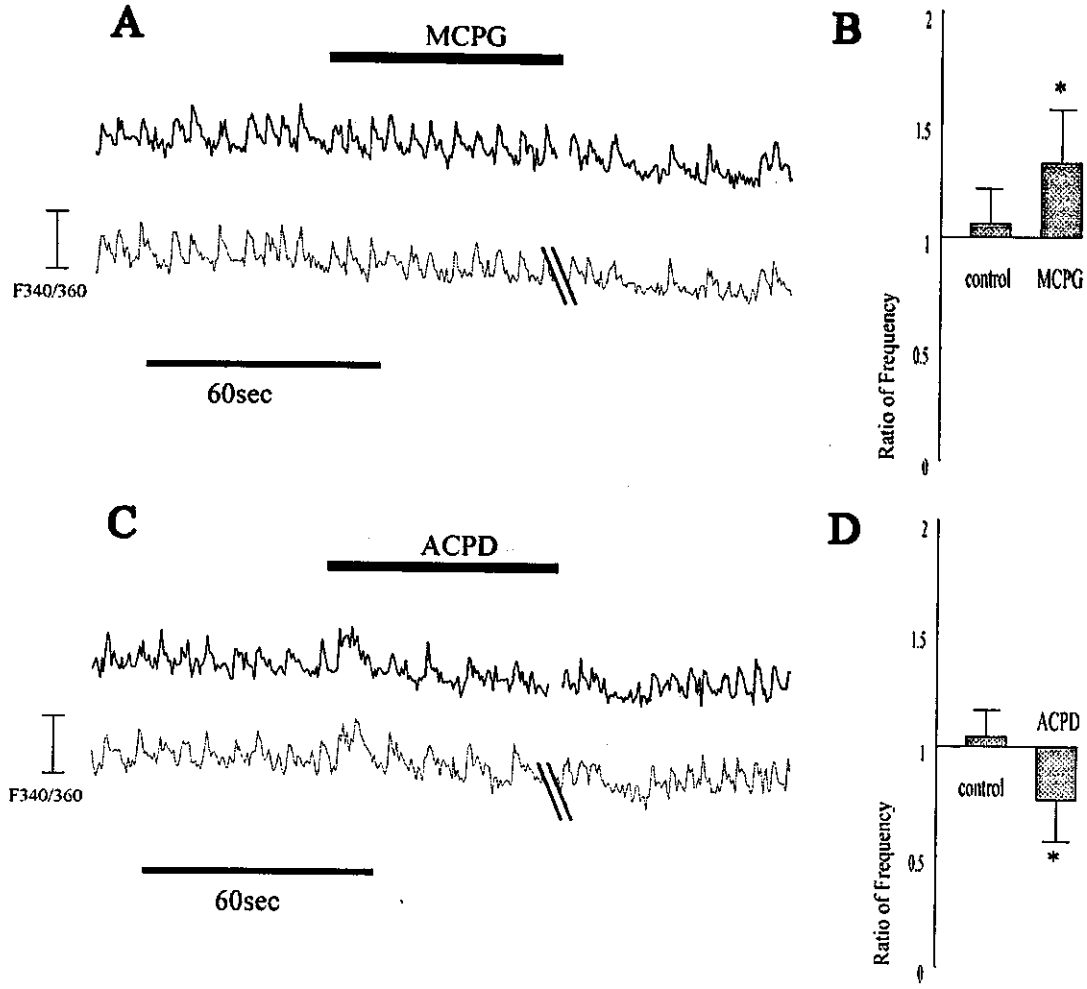

Fig. 2. Modulation of the frequency of spontaneous Ca^{2+} spikes by the mGluR signaling pathway. Increase and decrease in the frequency of the synchronized Ca^{2+} spike induced by MCPG (A) and ACPD (C), respectively. Traces of each figure show representative recordings of synchronized Ca^{2+} spikes in two cortical neurons randomly selected from the imaging fields under baseline and after bath-application of MCPG (500 μM) or ACPD (10 μM). The time gaps (//) of both figures were 90 s. Changes in the synchronized Ca^{2+} spike frequency induced by the application of MCPG (B) or ACPD (D). Data are presented as the mean ± SD ((B) control: 35 cells, MCPG: 42 cells; (D) control: 28 cells, ACPD: 42 cells). Asterisks indicate significance against the control ($p < 0.05$).

Inhibition of the cAMP Signaling Pathway Through Group II mGluR has Suppressive Effects on the Frequency of Synchronized Ca^{2+} Spikes

We next attempted to determine the subgroup-specific role of mGluRs in the frequency of synchronized Ca^{2+} spikes.

AIDA (100 μM) (Nc = 5, Nw = 7, 49/49cells, Fig. 3(A)) and PHCCC (30 μM) (Nc = 5, Nw = 6, 42/42cells, Fig. 3(B)), group I mGluR antagonists, did not affect the frequency of synchronized Ca^{2+} spikes. This result suggests that group I mGluR might have less involvement in the changes in frequency of synchronized Ca^{2+} spikes. On the other hand, EGLU (300 μM), a group II mGluR antagonist, induced a significant

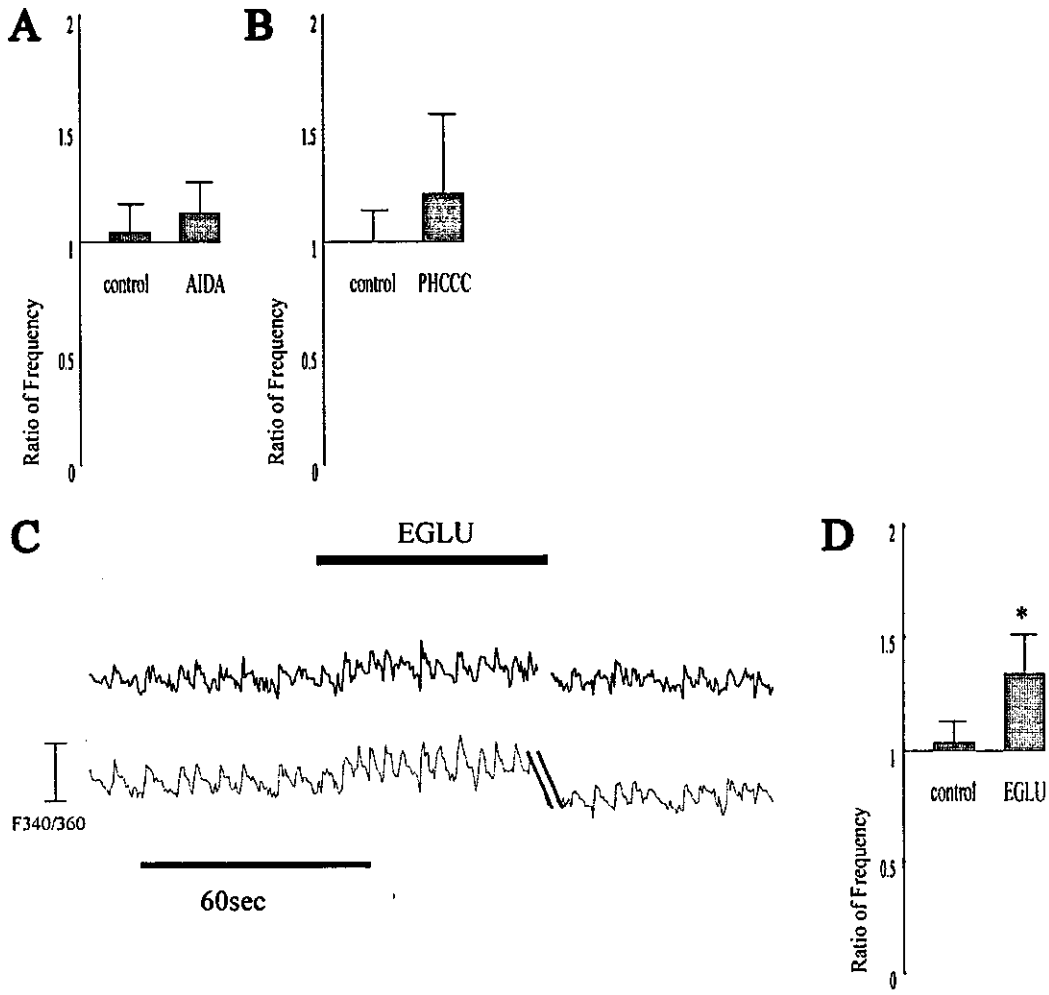

Fig. 3. Little involvement of the group I mGluR and large modulation of the group II mGluR in the frequency of spontaneous Ca^{2+} spikes. No changes in the synchronized Ca^{2+} spike frequencies in response to the application of AIDA (100 μM) (A) and to the application of PHCCC (30 μM). Data represent means ± SD ((A) control: 28 cells, AIDA: 49 cells; (B) control: 35 cells, PHCCC: 42 cells). (C) Increase in the frequency of the synchronized Ca^{2+} spike induced by EGLU. Traces show representative recordings in two cortical neurons under baseline and after bath-application of EGLU (300 μM). The time gap (//) was 135 s. (D) Changes in the synchronized Ca^{2+} spike frequency induced by the application of EGLU. Data represent means ± SD (control: 42 cells; EGLU: 42 cells); $*p < 0.05$ against control.

increase in the frequency of synchronized Ca^{2+} spikes (Nc = 5, Nw = 6, 42/42cells, Fig. 3(C) and (D)), suggesting that the suppressive effects of mGluRs on the frequency of synchronized Ca^{2+} spikes are mediated dominantly by group II mGluR. We confirmed the expression of group II mGluR by immunocytochemical staining (data not shown). MAP-2-positive primary cultured cortical neurons were found to express group II mGluRs at 8 DIV.

It is known that group II mGluR inhibits adenylate cyclase, resulting in a decrease in cAMP concentrations, and thereby inhibiting activation of protein kinase A (PKA) (Knopfel and Grandes, 2002). To verify the involvement of the cAMP pathway in the EGLU-induced increase in the frequency of synchronized Ca^{2+} spikes,

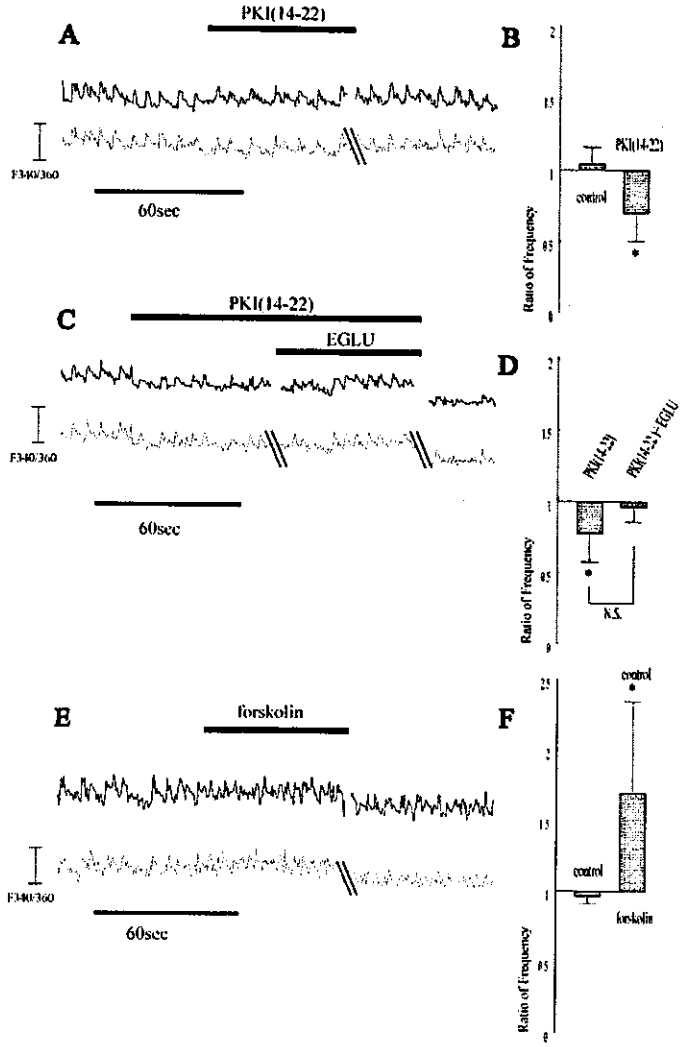

Fig. 4. Modulation of the frequency of spontaneous Ca^{2+} spikes by the PKA signaling pathway. (A) and (E) Decrease and increase in the frequency of the synchronized Ca^{2+} spike induced by PKI(14–22) and forskolin, respectively. Traces of each figure show representative recordings in two cortical neurons under baseline and after bath-applications of PKI(14–22) (100 μM) and forskolin (15 μM), respectively. The time gap (//) of each figure was 200 and 150 s, respectively. (B) and (F) Changes in the synchronized Ca^{2+} spike frequency induced by the application of PKI(14–22) or forskolin, respectively. Data represent means ± SD ((B) control: 28 cells, EGLU: 28 cells; (F) control: 28 cells, forskolin: 84 cells); $*p < 0.05$ against control. (C) EGLU failed to show significant increase in the frequency of synchronized Ca^{2+} spikes against control in the presence of PKI(14–22). Traces show representative recordings in two cortical neurons under baseline, application of PKI(14–22) (100 μM), and subsequent application of EGLU (300 μM). The time gaps (//) were 60 and 135 s. (D) No significant change in the synchronized Ca^{2+} spike frequency by the application of EGLU in the presence of PKI(14–22). Data represent means ± SD (PKI(14–22) and PKI(14–22) + EGLU (both bars): 42 cells); $*p < 0.05$ against control. N.S.: not significant.

we applied PKA inhibitor fragment 14–22 (PKI(14–22)). Application of PKI(14–22) (100 μM) alone was found to significantly reduce the frequency of spontaneous Ca^{2+} spikes (Nc = 4, Nw = 4, 28/28cells, Fig. 4(A) and (B)), suggesting that inactivation of PKA reduces the frequency of synchronized Ca^{2+} spikes. Furthermore, in the presence of PKI(14–22), subsequent application of EGLU failed to show a statistically significant increase in the frequency of synchronized Ca^{2+} spikes: increased the frequency slightly but not statistically significant, leaving it below the control level (Fig. 4(C) and (D)). This result indicated that the EGLU-induced increase in the Ca^{2+} spike frequency resulted from mainly through the activation of PKA by the blocking glutamate signals through group II mGluR. On the contrary, to investigate whether activation of the cAMP pathway was sufficient to increase the frequency of synchronized network Ca^{2+} spikes, we applied forskolin to activate adenylate cyclase to elevate intracellular cAMP levels. Forskolin (15 μM) greatly increased the synchronized Ca^{2+} spike frequency (Nc = 4, Nw = 12, 84/84cells, Fig. 4(E) and (F)), suggesting that the elevation in cAMP induced the increase in the frequency of the synchronized Ca^{2+} spikes. These results, in summary, indicate that the cAMP–PKA pathway plays a profound role in regulating of the frequency of the synchronized Ca^{2+} spikes in neural networks, and that glutamate signals, via group II mGluR, decrease the frequency of synchronized Ca^{2+} spikes through inactivation of the adenylate cyclase–cAMP–PKA pathway.

DISCUSSION

This study demonstrates an intriguing involvement of group II, but not group I, mGluR in spontaneously occurring synchronized Ca^{2+} spikes in cultured mouse cortical neurons.

We observed that the cultured mouse cortical neurons formed a neural network with synapses, and burst synchronously and periodically without any stimulation, which could be visualized as periodic and synchronous changes in the concentrations of intracellular Ca^{2+}. Pharmacological examinations using TTX revealed that these synchronized Ca^{2+} changes were accompanied by membrane depolarizations and action potentials in neurons, which was consistent with a previous report in rat cortical neurons (Robinson *et al.*, 1993). Periodical synchronized Ca^{2+} spikes of neurons in CNS accompanied by neural bursts is said to be essential for the development and differentiation of CNS (Garaschuk *et al.*, 1998; Gray *et al.*, 1989; Nakamura *et al.*, 1992). So, Ca^{2+} spikes in the present study can be considered as a good *in vitro* model of synchronized Ca^{2+} spikes in developing CNS.

The present results indicated that mGluRs, particularly group II mGluR, are involved in regulating the frequency of synchronized Ca^{2+} spikes in this neural networks, and that inactivation of adenylate cyclase, decrease in cAMP, and subsequent inactivation of PKA resulted in decrease in the spike frequency. However, even in the presence of PKA(14–22), EGLU induced slight but not significant increase in the frequency of Ca^{2+} spikes, leaving the frequency below the control level. There may be other pathways than cAMP–PKA cascade that regulate the frequency of synchronized Ca^{2+} spikes in downstream from group II mGluR.

A previous report has indicated that specific mGluR subgroups are differentially involved in synaptic plasticity and the modulation of hippocampal synaptic transmissions, and that group I mGluR plays a role in both LTD and LTP, whereas group II mGluR is involved only in LTD induction (Manahan-Vaughan, 1997). Suppressive effects of group II mGluR and little effects of group I mGluR on the frequency of synchronized Ca^{2+} spikes, appeared to correspond to the effects that group II mGluR induce LTD and group I mGluR induce both LTD and LTP in synaptic transmission. It has been considered that involvements of mGluRs in LTD and LTP relate to an important system by which the efficacy of synaptic transmission is regulated. Thus, regulation of the frequency of synchronized Ca^{2+} spikes by mGluRs might also reflect changes of the efficacy of synaptic transmission.

We have reported the importance of mGluRs in regulating of the frequency of synchronized Ca^{2+} spikes in cultured cortical neurons. Still, it remains possible that astrocytes and/or other glial cells are concerned with changes in the frequency of synchronized Ca^{2+} spikes. Glial cells expressing mGluRs might be activated by glutamate released by neurons, and then indirectly regulate the frequency of neural Ca^{2+} spikes. Some reports have indicated that glutamate acting on mGluRs increases intracellular Ca^{2+} concentrations in astrocytes (Guiramand *et al.*, 1991; Jensen and Chiu, 1990) in addition to neurons (Courtney *et al.*, 1990; Llano *et al.*, 1991). However, changes in the frequency of synchronized Ca^{2+} spikes according to the activation of the mGluRs in this report were changes of neural Ca^{2+} spikes, because they were accompanied by action potentials, and small cell bodies of neurons visualized by fura-2 apparently differed from the flat, practically invisible in the present experiments, morphology of astrocytes (Suzuki *et al.*, 2003).

Previous reports have verified that iGluRs have an operative function in synchronized Ca^{2+} spikes. Here, we propose that group II mGluR via inactivation of the cAMP signaling pathway has a "modulative" function in the regulating the frequency of synchronized Ca^{2+} spikes. Interestingly, glutamate, the most major excitatory neurotransmitter, was found to simultaneously generate the synchronized Ca^{2+} spikes and modulate their frequency, in the present *in vitro* neural network.

We believe that glutamate signals through group II mGluR modulate the efficacy of synaptic transmissions, which is important not only during CNS development but for memory and neuroplasticity in adulthood.

REFERENCES

Aguirre, J. A., Andbjer, B., Gonzalez-Baron, S., Hansson, A., Stromberg, I., Agnati, L. F., and Fuxe, K. (2001). Group I mGluR antagonist AIDA protects nigral DA cells from MPTP-induced injury. *Neuroreport* **12**:2615–2617.

Akasu, T., and Tokimasa, T. (1989). Potassium currents in submucous neurones of guinea-pig caecum and their synaptic modification. *J. Physiol. (Lond.)* **416**:571–588.

Bacci, A., Verderio, C., Pravettoni, E., and Matteoli, M. (1999). Synaptic and intrinsic mechanisms shape synchronous oscillations in hippocampal neurons in culture. *Eur. J. Neurosci.* **11**:389–397.

Courtney, M. J., Lambert, J. J., and Nicholls, D. G. (1990). The interactions between plasma membrane depolarization and glutamate receptor activation in the regulation of cytoplasmic free calcium in cultured cerebellar granule cells. *J. Neurosci.* **10**:3873-3879.

Garaschuk, O., Hanse, E., and Konnerth, A. (1998). Developmental profile and synaptic origin of early network oscillations in the CA1 region of rat neonatal hippocampus. *J. Physiol. (Lond.)* **507**:219–236.

Gray, C. M., Konig, P., Engel, A. K., and Singer, W. (1989). Oscillatory responses in cat visual cortex exhibit inter-columnar synchronization which reflects global stimulus properties. *Nature* **338**:334–337.

Guiramand, J., Vignes, M., and Recasens, M. (1991). A specific transduction mechanism for the glutamate action on phosphoinositide metabolism via the quisqualate metabotropic receptor in rat brain synaptoneurosomes: II. Calcium dependency, cadmium inhibition. *J. Neurochem.* **57**:1501–1509.

Ichikawa, M., Muramoto, K., Kobayashi, K., Kawahara, M., and Kuroda, Y. (1993). Formation and maturation of synapses in primary cultures of rat cerebral cortical cells: An electron microscopic study. *Neurosci. Res. Suppl.* **16**:95–103.

Jensen, A. M., and Chiu, S. Y. (1990). Fluorescence measurement of changes in intracellular calcium induced by excitatory amino acids in cultured cortical astrocytes. *J. Neurosci.* **10**:1165–1175.

Kalda, A., Kaasik, A., Vassiljev, V., Pokk, P., and Zharkovsky, A. (2000). Neuroprotective action of group I metabotropic glutamate receptor agonists against oxygen–glucose deprivation-induced neuronal death. *Brain Res.* **853**:370–373.

Knopfel, T., and Grandes, P. (2002). Metabotropic glutamate receptors in the cerebellum with a focus on their function in Purkinje cells. *Cerebellum* **1**:19–26.

Kuroda, Y., Ichikawa, M., Muramoto, K., Kobayashi, K., Matsuda, Y., Ogura, A., and Kudo, Y. (1992). Block of synapse formation between cerebral cortical neurons by a protein kinase inhibitor. *Neurosci. Lett.* **135**:255–258.

Llano, I., Dreessen, J., Kano, M., and Konnerth, A. (1991). Intradendritic release of calcium induced by glutamate in cerebellar Purkinje cells. *Neuron* **7**:577–583.

Maj, M., Bruno, V., Dragic, Z., Yamamoto, R., Battaglia, G., Inderbitzin, W., Stoehr, N., Stein, T., Gasparini, F., Vranesic, I., Kuhn, R., Nicoletti, F., and Flor, P. J. (2003). (–)-PHCCC, a positive allosteric modulator of mGluR4: Characterization, mechanism of action, and neuroprotection. *Neuropharmacology* **45**:895–906.

Manahan-Vaughan, D. (1997). Group 1 and 2 metabotropic glutamate receptors play differential roles in hippocampal long-term depression and long-term potentiation in freely moving rats. *J. Neurosci.* **17**:3303–3311.

Mao, L., and Wang, J. Q. (2001a). Upregulation of preprodynorphin and preproenkephalin mRNA expression by selective activation of group I metabotropic glutamate receptors in characterized primary cultures of rat striatal neurons. *Brain Res. Mol. Brain* **86**:125–137.

Mao, L., and Wang, J. Q. (2001b). Selective activation of group I metabotropic glutamate receptors upregulates preprodynorphin, substance P, and preproenkephalin mRNA expression in rat dorsal striatum. *Synapse* **39**:82–94.

Marti, M., Paganini, F., Stocchi, S., Bianchi, C., Beani, L., and Morari, M. (2001). Presynaptic group I and II metabotropic glutamate receptors oppositely modulate striatal acetylcholine release. *Eur. J. Neurosci.* **14**:1181–1184.

Meli, E., Picca, R., Attucci, S., Cozzi, A., Peruginelli, F., Moroni, F., and Pellegrini-Giampietro, D. E. (2002). Activation of mGlu1 but not mGlu5 metabotropic glutamate receptors contributes to postischemic neuronal injury in vitro and in vivo. *Pharmacol. Biochem. Behav.* **73**:439–446.

Nakamura, K., Mikami, A., and Kubota, K. (1992). Oscillatory neuronal activity related to visual short-term memory in monkey temporal pole. *Neuroreport* **3**:117–120.

Nakanishi, S. (1992). Molecular diversity of glutamate receptors and implications for brain function. *Science* **258**:597–603.

Numakawa, T., Yamagishi, S., Adachi, N., Matsumoto, T., Yokomaku, D., Yamada, M., and Hatanaka, H. (2002). Brain-derived neurotrophic factor-induced potentiation of Ca(2+) oscillations in developing cortical neurons. *J. Biol. Chem.* **277**:6520–6529.

Ogura, A., Iijima, T., Amano, T., and Kudo, Y. (1987). Optical monitoring of excitatory synaptic activity between cultured hippocampal neurons by a multi-site $Ca2^{+}$ fluorometry. *Neurosci. Lett.* **78**:69–74.

Pin, J. P., and Duvoisin, R. (1995). The metabotropic glutamate receptors: Structure and functions. *Neuropharmacology* **34**:1-26.

Przewlocki, R., Parsons, K. L., Sweeney, D. D., Trotter, C., Netzeband, J. G., Siggins, G. R., and Gruol, D. L. (1999). Opioid enhancement of calcium oscillations and burst events involving NMDA receptors and L-type calcium channels in cultured hippocampal neurons. *J. Neurosci.* **19**:9705–9715.

Robinson, H. P., Kawahara, M., Jimbo, Y., Torimitsu, K., Kuroda, Y., and Kawana, A. (1993). Periodic synchronized bursting and intracellular calcium transients elicited by low magnesium in cultured cortical neurons. *J. Neurophysiol.* **70**:1606–1616.

Schoepp, D. D., Jane, D. E., and Monn, J. A. (1999). Pharmacological agents acting at subtypes of metabotropic glutamate receptors. *Neuropharmacology* **38**:1431–1476.

Schwarz, D. W., Tennigkeit, F., and Puil, E. (2000). Metabotropic transmitter actions in auditory thalamus. *Acta Otolaryngol. (Stockh.)* **120**:251–254.

Sluka, K. A. (1997). Activation of the cAMP transduction cascade contributes to the mechanical hyperalgesia and allodynia induced by intradermal injection of capsaicin. *Br. J. Pharmacol.* **122**:1165–1173.

Suzuki, R., Watanabe, J., Arata, S., Funahashi, H., Kikuyama, S., and Shioda, S. (2003). A transgenic mouse model for the detailed morphological study of astrocytes. *Neurosci. Res.* **47**:451–454.

Thornton, P. D., and Bornstein, J. C. (2002). Slow excitatory synaptic potentials evoked by distension in myenteric descending interneurones of guinea-pig ileum. *J. Physiol. (Lond.)* **539**:589–602.

Verderio, C., Bacci, A., Coco, S., Pravettoni, E., Fumagalli, G., and Matteoli, M. (1999). Astrocytes are required for the oscillatory activity in cultured hippocampal neurons. *Eur. J. Neurosci.* **11**:2793–2800.

Yasumoto, F., Negishi, T., Ishii, Y., Kyuwa, S., Kuroda, Y., and Yoshikawa, Y. (2004). Endogenous dopamine maintains synchronous oscillation of intracellular calcium in primary cultured-mouse midbrain neurons. *Cell. Mol. Neurobiol.* **24**:51–61.

Zhou, S., Komak, S., Du, J., and Carlton, S. M. (2001). Metabotropic glutamate 1alpha receptors on peripheral primary afferent fibers: Their role in nociception. *Brain Res.* **913**:18–26.

Placenta (2005), 26, 99–103
doi:10.1016/j.placenta.2004.05.007

SHORT COMMUNICATION

Localization of Ubiquitin Carboxyl-terminal Hydrolase-L1 in Cynomolgus Monkey Placentas

S. Sekiguchi[a,*], A. Takatori[a], T. Negishi[a], J. Kwon[a,b], T. Kokubo[c], Y. Ishii[a], S. Kyuwa[a] and Y. Yoshikawa[a]

[a] Department of Biomedical Science, Graduate School of Agricultural and Life Sciences, University of Tokyo, 1-1-1 Yayoi, Bunkyo-ku, Tokyo 113-8657, Japan; [b] Department of Degenerative Neurological Disease, National Institute of Neuroscience, National Center of Neurology and Psychiatry, Kodaira, Tokyo 187-8502, Japan; [c] Fuji Photo Film Co., Ltd., Environmental Protection & Products Safety Division Material Safety Test Center, 210, Nakanuma, Minamiashigara-shi, Kanagawa 250-0193 Japan

Paper accepted 17 May 2004

Ubiquitin carboxyl-terminal hydrolase-L1 (UCH-L1) is a restrictedly expressed enzyme in neural and reproductive tissues, and it is considered to have a significant role in reproduction. In the present study, we investigated the localization of UCH-L1 in placenta of cynomolgus monkeys (*Macaca fascicularis*). UCH-L1 protein was detected in cytotrophoblasts of chorionic plate and villi, and decidual cells of decidua basalis in cynomolgus monkey placenta, and the amount of UCH-L1 protein in whole placenta increased as pregnancy progressed. These results supported that UCH-L1 is necessary for placental and fetal development in primate placenta. This is the first report to demonstrate the presence of UCH-L1 in primate placenta, and the cynomolgus monkey may be a useful model for the study of the functions of the ubiquitin–proteasome system in human pregnancy.
Placenta (2005), 26, 99–103

INTRODUCTION

The ubiquitin–proteasome system is a major pathway for protein degradation in eukaryotic cells [1]. This pathway uses the ubiquitin protein as a marker for intracellular protein processed by rapid proteolysis via a multi-subunit protease complex, the proteasome [2]. The ubiquitin-mediated degradation of certain regulatory proteins is considered to play a number of critical roles in cell-specific functions, including the cell cycle [3], apoptosis [4], inflammatory responses, and antigen presentation [5]. Attachment of ubiquitin to a target protein, referred to as ubiquitination, is a complex ATP-dependent process carried out by the ubiquitin-activating enzyme (E1), the ubiquitin-conjugating enzyme (E2) and ubiquitin ligase (E3) [6].

This pathway is considered to be important for placental growth and development. In previous studies, ubiquitin was detected in cytotrophoblasts in human placenta [7], and it has also been detected in decidual cells during pregnancy in the human uterus, although endometrial stromal cells in the non-pregnant uterus are known to have low concentrations of ubiquitin [8,9]. In vitro, human decidual cells have been shown to secrete ubiquitin [10]. In mice lacking the *UbcM4* gene encoding the E2 enzyme, multiple developmental abnormalities, such as a reduction in placental size, a thin chorionic plate, and scarce fetal blood vessels in the labyrinth, have been observed [11].

Ubiquitin carboxyl-terminal hydrolases (UCHs) are known to be de-ubiquitinating enzymes which recycle free ubiquitin from ubiquitin/protein complexes or polyubiquitin chains by cleaving the amide linkage neighboring the C-terminal glycine of ubiquitin [12]. UCH-L1, a member of the UCH family, is one of the most abundant soluble proteins in the brain (1–5% of the total soluble protein). Previous immunohistochemical studies have demonstrated that UCH-L1 is expressed exclusively in neuronal tissue [13–16], but it has also been reported in reproductive tissues such as spermatogonia and Sertoli cells in mice [15,17,18], spermatogonia in monkeys [19] and oocytes in mice [15]. Previous studies have also reported that gracile axonal dystrophy (gad) mutant mice, which lack UCH-L1, showed neuroaxonal dystrophy in the gracile nucleus of the medulla and the gracile fascicules of the spinal cord

* Corresponding author. Tel.: +81-3-5841-5038; fax: +81-3-5841-8186.
E-mail address: aa37162@mail.ecc.u-tokyo.ac.jp (S. Sekiguchi).

0143–4004/$–see front matter

[20–22]. In reproductive tissue, male gad mice exhibited a deterioration of spermatogenesis with aging [17]. Moreover, litter size in female gad mice was significantly lower than that in normal female mice, a finding which was independent of the genotype of the male partner [23]. We previously demonstrated the expression of UCH-L1 protein in decidual cells in the mouse placenta [24]. These results, when taken together, suggest that active UCH-L1 is necessary for normal reproductive processes to take place.

In the present study, we investigated the expression of UCH-L1, ubiquitin, and PCNA protein in the placenta of cynomolgus monkeys at three different gestational stages (50, 80, and 120 days of gestation), and we demonstrated the localization of UCH-L1 protein in cytotrophoblasts of the chorionic plate and villi, and in the decidual cells of the decidua basalis in the cynomolgus monkey placenta at all stages.

MATERIALS AND METHODS

Animals

Six pregnant cynomolgus monkeys (*Macaca fascicularis*) at gestational day (GD) 50, 80, and 120 ($n = 2$/each stage) were purchased from Shin Nippon Biomedical Laboratories, Ltd., and four monkeys at GD 83, 84, 93, and 102 were obtained from the Tsukuba Primate Center, National Institute of Infectious Diseases, Japan. The placentas were obtained by caesarean operation.

A piece of placenta at GD 50, 80, and 120 was fixed in 4% paraformaldehyde and embedded in paraffin for the immunohistochemical studies. The remaining placenta at GD 50, 80, and 120, as well as four whole placentas at GD 83, 84, 93, and 102 were subjected to Western blot analysis (see below).

Antibodies

A rabbit polyclonal antibody against protein gene product (PGP) 9.5 (PGP9.5; UltraClone Limited, England) was used for detecting UCH-L1. PGP 9.5 is equivalent to UCH-L1, and antibody against PGP 9.5/UCH-L1 is now widely used for investigation of the central and peripheral nervous systems. A rabbit polyclonal antibody against ubiquitin (Ubiquitin; DAKO, Denmark), and a mouse monoclonal antibody against proliferating cell nuclear antigen (PCNA; DAKO, Denmark) were used for detecting ubiquitin and proliferative activity of the cells, respectively.

Immunohistochemistry

Deparaffinized sections were pretreated with 0.3% H_2O_2 in methanol for 30 min for the inactivation of endogenous peroxidase and the sections were washed in phosphate buffer saline (PBS). Non-specific binding of immunoglobulins was blocked by incubation with Block Ace (Dainippon Pharmaceutical, Ltd., Japan) for 1 h at room temperature. The sections were then incubated with primary antibodies against PGP 9.5 (1:8000), ubiquitin (1:500), and PCNA (1:1000) for 16 h at 4 °C. The sections were then incubated with either biotinylated goat anti-rabbit or goat anti-mouse IgG (1:500; DAKO, Denmark), which was followed by incubation with streptavidin–biotin–horseradish peroxidase complex (sABC kit; DAKO, Denmark). The immunoreactive elements were visualized by treating the sections with 3,3′-diaminobenzidine tetroxide (Dojin Kagaku, Japan). Finally, the sections were counterstained with hematoxylin. The regions of placenta examined in this study included the chorionic plate, chorionic villi, cell columns, cytotrophoblastic shell, and decidua basalis. Negative control sections were incubated with non-immunized rabbit or mouse serum as substitutes for the primary antibody.

Western blot analysis

Placental tissue (5 g) was homogenized and fractionated into microsome fractions. The samples (20 μg of total protein) were electrophoresed by 15% SDS-PAGE. The separated proteins in the gels were transferred and blotted onto polyvinylidene fluoride membranes (Immobilon P; Millipore, Bedford, MA). After blocking the membranes with 5% nonfat dried milk in 20 mM phosphate buffer saline (pH 7.0) and 0.1% Tween-20 overnight at 4 °C, the blotted membranes were incubated with primary antibody (PGP 9.5; diluted at 1:15,000) for 1 h at room temperature. The membranes were then incubated with horseradish peroxidase conjugated goat anti-rabbit IgG (1:50,000, Jackson Lab, West Grove, PA) for 1 h at room temperature. Immunoreactions were visualized by enhanced chemiluminescence (ECL plus, Amersham, UK). Immunoreactive bands obtained from the Western blots were quantified using commercially available software (Quantity One; PDI, Upper Saddle River, NJ).

RESULTS

At all three stages, UCH-L1 protein was intensely and diffusely expressed in the cytoplasm and nuclei of the cytotrophoblasts of the chorionic plate and villi (Figure 1A–C). As regards the intensity of the immunoreaction of UCH-L1 in the cytotrophoblasts, no difference was observed among the three stages, but the number of chorionic villi increased markedly as the gestational days passed. At GD 50 and 80, ubiquitin protein was diffusely expressed in the cytoplasm and nuclei of the cytotrophoblasts and stromal cells, and only in the nuclei of the syncytiotrophoblasts of the chorionic villi (Figure 1D). At GD 120, ubiquitin protein was expressed in the cytoplasm and nuclei of the cytotrophoblasts and stromal cells, but only in the nuclei of syncytiotrophoblasts. PCNA protein was expressed in the cytotrophoblasts and stromal cells of the chorionic plate and villi at all three stages (data not shown).

UCH-L1 protein was not expressed in the cytotrophoblasts of the cell columns and cytotrophoblastic shell (Figure 1E and F), although ubiquitin protein was diffusely expressed in the cytoplasm and nuclei of the cytotrophoblasts at all three stages (Figure 1G and H). PCNA protein was expressed in the cytotrophoblasts in the cell columns and cytotrophoblastic shell at all three stages (Figure 1I and J).

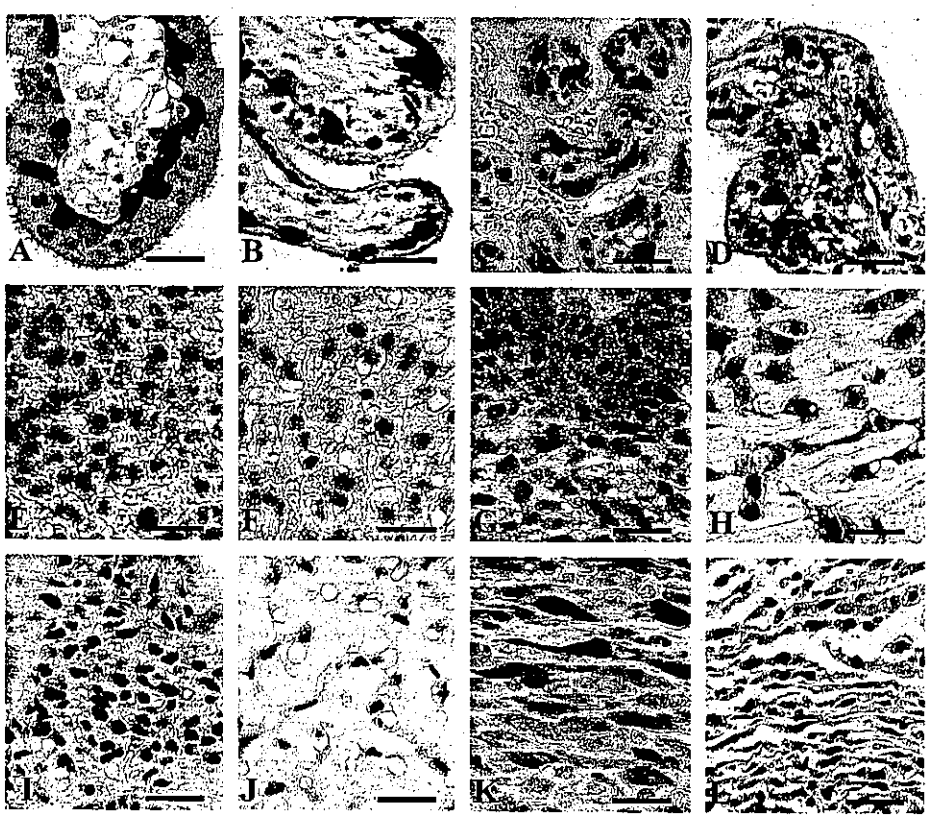

Figure 1. Immunohistochemistry of chorionic villi (A–D), cell columns (E, G and I), cytotrophoblastic shell (F, H and J) and decidua basalis (K and L) of cynomolgus monkey placenta against UCH-L1 (A–C, E, F and K), ubiquitin (D, G, H and L) and PCNA (I and J). UCH-L1 is detected in cytotrophoblasts of chorionic villi at gestational day (GD) 50 (A), 80 (B) and 120 (C), and in decidual cells at GD 80 (K), not in cytotrophoblasts of cell columns and cytotrophoblastic shell at GD 80 (E and F). Ubiquitin is detected in cytotrophoblasts, syncytiotrophoblasts and stromal cells of chorionic villi at GD 80 (D), cytotrophoblasts of cell columns and cytotrophoblastic shell at GD 80 (G and H), and decidua basalis at GD 80 (L). PCNA is detected in cytotrophoblasts of cell columns and cytotrophoblastic shell at GD 80 (I and J). Scale bar: 25 μm.

In the decidua basalis, UCH-L1 and ubiquitin protein were diffusely expressed in the cytoplasm and nuclei of decidual cells (Figure 1K and L). The intensity of the UCH-L1 immunoreaction in the decidual cells varied; these cells exhibited a mixed pattern at all three stages, i.e., some were intensely stained, while others were only slightly stained. The ubiquitin immunoreaction in the nuclei was more intense than in the cytoplasm of the decidual cells at all three stages. PCNA protein was expressed in the decidual cells at all three stages (data not shown).

Western blot analysis

Western blot analysis revealed that UCH-L1 protein was expressed in the placenta at all the stages of pregnancy (Figure 2A). The expression of UCH-L1 increased significantly ($p < 0.0001$) as pregnancy progressed (Figure 2B).

DISCUSSION

In the present study, we demonstrated the localization of UCH-L1 protein in the placenta of cynomolgus monkeys at three gestational stages for the first time. UCH-L1-, ubiquitin-, and PCNA-positive cytotrophoblasts were observed in the chorionic plate and villi at all stages.

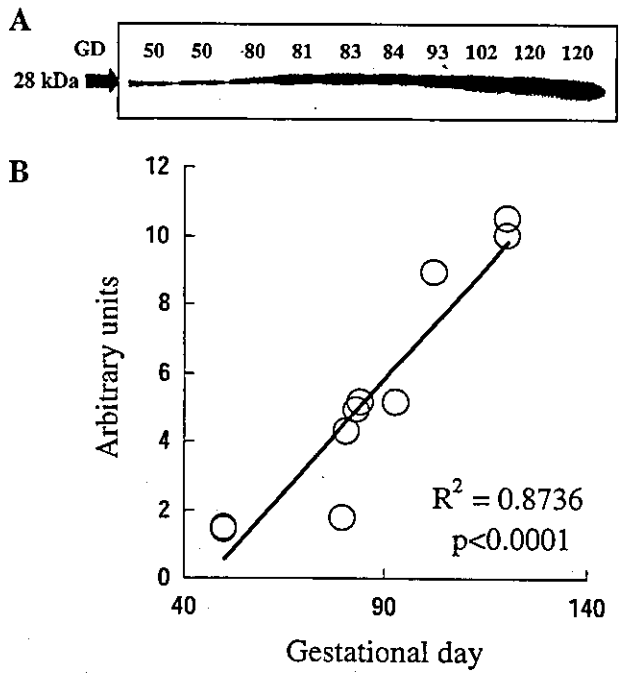

Figure 2. Analysis of UCH-L1 expression in cynomolgus monkey placentas. A 28 kDa band is detected in placentas at all gestational days (GD) (A). The expression of UCH-L1 increases significantly as pregnancy progresses (B).